Polycrystalline CVD Diamond Films with High Electrical Mobility

M. A. Plano, M. I. Landstrass, L. S. Pan, S. Han, D. R. Kania, S. McWilliams, J. W. Ager III

Advances in the deposition process have led to dramatic improvements in the electronic properties of polycrystalline diamond films produced by chemical vapor deposition (CVD). It is now possible to produce CVD diamond with properties approaching those of IIa natural diamonds. The combined electron-hole mobility, as measured by transient photoconductivity at low carrier density, is 4000 square centimeters per volt per second at an electric field of 200 volts per centimeter and is comparable to that of the best single-crystal IIa natural diamonds. Carrier lifetimes measured under the same conditions are 150 picoseconds for the CVD diamond and 300 picoseconds for single-crystal diamond. The collection distance at a field of 10 kilovolts per centimeter is 15 micrometers for the CVD diamond as compared to 30 micrometers for natural diamonds. The electrical qualities appear to correlate with the width of the diamond Raman peak. Also, although the collection distance at the highest fields in the films nearly equals the average grain size, there is no evidence of deleterious grain boundary effects.

Because of its large bandgap, high electron and hole saturation velocities, high mobilities, high breakdown strength, and high radiation hardness, diamond has been proposed for a wide variety of electronic applications, particularly those involving extreme conditions (*1–4*). Some research in this area has focused on prototype systems based on natural or homoepitaxial single-crystal diamond (*5–9*). However, polycrystalline CVD diamond films, which can be grown over large areas on nondiamond substrates such as silicon, represent an alternate medium for research and development of both active and passive diamond electronic applications (*10*).

To date, the electronic performance of CVD diamond films has been inferior to that of the highest quality single-crystal natural IIa diamond. Polycrystalline CVD diamond films with combined electron and hole mobilities of 50 $\text{cm}^2\ \text{V}^{-1}\ \text{s}^{-1}$ and lifetimes of 50 ps have been reported (*11*). Further development of diamond films for applications that require high thermal conductivity resulted in material with mobilities of 1000 $\text{cm}^2\ \text{V}^{-1}\ \text{s}^{-1}$ and lifetimes of 100 ps (*12*). In this report we describe polycrystalline diamond films that have combined electron and hole mobilities of 4000 $\text{cm}^2\ \text{V}^{-1}\ \text{s}^{-1}$ and carrier lifetimes of 150 ps, properties that approach those of the best IIa diamonds. We compare measurements of the combined mobility, drift velocity, lifetime, and collection distance to those of other CVD films and to natural diamond. Such high-quality CVD polycrystalline diamond, because of its manufacturing flexibility and low cost, may make it possible to develop diamond devices that otherwise would have been too expensive or impractical with single-crystal diamond.

The polycrystalline diamond films were grown on silicon substrates in a microwave (*13*) CVD plasma reactor that used methane, carbon monoxide (*14*), and hydrogen gases. The important growth parameters were systematically varied to determine the process for growth of high-quality diamond. These parameters include microwave power, pressure, gas mixture, and growth temperature. Raman spectroscopy was used as a first step in determining the success of a particular process. Scanning electron micrographs were used to study the surface morphology and to measure the grain size of the films. The ultimate tests of the process were the mobility and lifetime of the free carriers measured with transient photoconductivity (PC) (*11*).

With transient PC, one measures the mobility (μ), the lifetime (t), and the average collection distance (d) of free carriers by following the changing current associated with the absorption of light. The free carriers are intrinsically excited by a 5-ps pulse of 6.1-eV photons. The absorption depth at this energy is less than 2 μm. Electrical contacts to the samples are made by sputtering a 1-mm-wide line of titanium and gold. A gap in the line defines the active region of the test structure. The current-voltage relation in the dark is linear for these structures. After the absorption of the light pulse, the transient decay of the PC is measured with a high-speed measurement system that has a resolution of 50 ps. This technique has been used on natural IIa diamonds (*15, 16*) and on earlier sets of diamond films (*11, 12*).

To illustrate the dramatic improvement, we will discuss three sets of diamond films. Films grown in mid-1990 to late 1991 will be labeled film A; films grown in late 1991, which were developed for use in thermal management, will be labeled film B (*12, 17*); and the most recent films, grown specifically for electronic applications, will be labeled film C. The process conditions for these three film types are shown in Table 1. The improvement in electrical behavior from film A to film C correlates with increased grain size, higher growth temperatures, and improved purity of the diamond films.

Raman spectroscopy is one of the most commonly used techniques for characterizing diamond films because of its high sensitivity to various phases of carbon bonding. Spectra from all three CVD diamond films were recorded. All of the CVD films display the characteristic diamond peak at 1332 cm^{-1}. Film C has the narrowest diamond peak with a full width at half maximum (FWHM) of 3.3 cm^{-1} compared to about 2.4 cm^{-1} for a IIa diamond. The FWHMs for the three films are listed in Table 2. The amount of non–diamond-bonded carbon that would contribute a broad peak at 1550 cm^{-1} is negligible in all three films.

A representative scanning electron micrograph of film C is shown in Fig. 1. We determined the average grain size by counting the number of grains in a region, dividing the area of the region by the number of grains, and taking the square root. Film C has average grain sizes of 14 to 16 μm, film B 10 to 12 μm, and film A 3 to 6 μm. The grain size is dependent on the process chemistry, the growth temperature, and the thickness of the film. If the process causes continuous renucleation, the resultant grain size is generally smaller. Owing to the competitive growth of the columnar grains, the grain size increases with thickness (*18*). The difference in grain size between film A and the other films is due mostly to thickness; temperature and chemistry account for the dif-

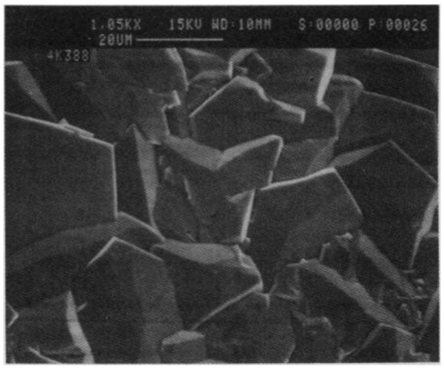

Fig. 1. Scanning electron micrograph of the morphology and grain size of high electrical quality CVD diamond (film C).

M. A. Plano, M. I. Landstrass, D. R. Kania, S. McWilliams, Crystallume, 125 Constitution Drive, Menlo Park, CA 94025.
L. S. Pan and S. Han, Lawrence Livermore National Laboratory, L-476, 7000 East Avenue, Livermore, CA 94550.
J. W. Ager III, Lawrence Berkeley Laboratory, University of California, Berkeley, CA 94720.

ferences observed between film B and film C.

The mobility was measured as a function of excited carrier density for the three sets of CVD diamond films and a IIa diamond (Fig. 2). The carrier density is calculated from the amount of absorbed energy, the volume of excitation, and the photon energy. The mobility decreases with density because of increased scattering between the electron and hole populations (*15*). At low densities, in all cases, the mobility saturates and becomes independent of the carrier density. Temperature-dependent measurements in IIa diamond have shown that the mobility scales as $\sim T^{-3/2}$ (*15*), indicating that the mobility is limited mainly by acoustic phonon scattering. These values for the mobility at low excitation densities (~ 4000 cm^2 V^{-1} s^{-1} at $n \leq 10^{15}$ cm^{-3}) at an applied electric field of 200 V cm^{-1} are higher than those reported in the past for either electrons or holes alone (*8*). However, PC measures a weighted sum of both electron and hole motion, and thus these values suggest that both electrons and holes contribute to the current flow.

Decay times of the transient are a measure of the lifetime of the free carriers. In film A, these times were short (<50 ps) and independent of the excitation density (*11*). For films B and C the decay times at low excitation density have values of 50 and 150 ps, respectively. In IIa diamonds the decay time varies from 100 to 400 ps, depending on the sample. For the IIa diamond discussed here the decay time is 300 ps at low excitation densities. The decay times for all films and natural diamond examined to date show a rapid decrease as the electric field increases and approaches a constant for fields greater than 2000 V cm^{-1}. This finding is unexplained at present.

In the development of applications such as radiation detectors, another important parameter is the collection distance *d* of the free carriers. This distance determines the sensitivity of the detector. Recent Monte Carlo work (*3*) indicates that a prototype multilayer sampling calorimeter detector would require a minimum collection distance of 25 μm. Typical operating electric fields for such detectors would be 30 to 40 kV cm^{-1}. A plot of the collection distance versus electric field for films B and C and the natural diamond is shown in Fig. 3. In film A (not shown) the distance never exceeded 0.1 μm. At a field of 10 kV cm^{-1}, which was the limit of the PC system, this distance was 2 μm in film B. At the same field, in film C the distance is between 15 and 20 μm, whereas in natural diamond the distance is almost 30 μm. These results indicate that films of quality equal to type C are suitable for detectors, particularly if operated at higher fields.

Throughout the development process the carrier mobility in CVD films has been continuously improved. Film C has a combined mobility equal to that of IIa diamond (4000 cm^2 V^{-1} s^{-1} at low carrier density). The lifetime *t*, although improved as well, has not shown so dramatic an increase and presently accounts for the lower collection distances shown in Fig. 3. At present, it is about half that of the IIa diamond (150 ps versus 300 ps). The much shorter lifetimes found in lower mobility CVD films can be attributed to trapping at a variety of defects known to be present in low-quality films: dislocations, stacking faults, impurities, and twins. It is possible that the longer carrier lifetime found in film C compared to earlier CVD films is the result of a lower density of defects but that the overall defect density is still somewhat higher than that in IIa natural diamonds.

Examination of the Raman spectra of CVD films used here and in previous studies (*11*) reveals a relation between the Raman spectrum and the electrical properties. Films with narrower Raman line shapes and low sp^2/sp^3 ratios (as measured by the peak at about 1500 cm^{-1}) tend to have larger combined mobilities and thus a larger collection distance. Although the mobilities of film C and the IIa diamond are identical, the diamond phonon FWHM is still somewhat larger in the CVD film than in the IIa diamond (3.3 cm^{-1} versus 2.4 cm^{-1}). A relatively narrow diamond linewidth appears to be a necessary but not sufficient condition for a high-mobility CVD film, and in high-mobility films carrier lifetime is inversely related to the Raman linewidth.

In CVD films, the linewidth has been linked to the phonon domain size (*19, 20*) and to inhomogeneous stress distributions (*20*). The rough relation between Raman FWHM and electrical properties suggests that the linewidth may be related to the defect density. The Raman linewidth in CVD diamond is determined, as it is in single-crystal material, by the lifetime of the optical phonon created in the Raman process, and it is possible that the symmetry constraints of this process ($\Delta k = 0$) may be relaxed at the defects, leading to shorter optical phonon lifetimes in CVD material and broader line shapes.

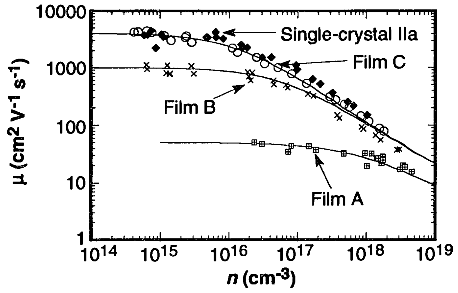

Fig. 2. Mobility measured with intrinsic PC for films A, B, and C and a IIa diamond. The mobility falls off at high densities as a result of electron-hole scattering. The solid lines are calculated mobilities based on electron-hole scattering.

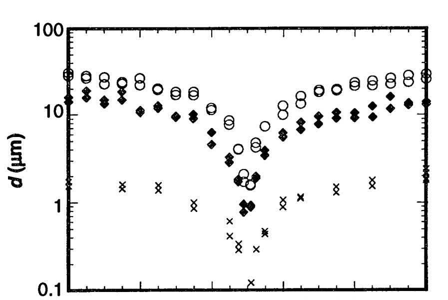

Fig. 3. Collection distance as a function of electric field for films B (×) and C (◆) and a IIa diamond (○). The collection distance of film C approaches that of the IIa diamond with the difference in performance due to shorter lifetimes in the CVD film.

Table 1. Microwave deposition parameters.

Sample	Substrate temperature (°C)	Pressure (torr)	Microwave power (W)	Microwave frequency (GHz)	Methane concentration (%)
Film A	650	50	1000	2.45	0.1
Film B	700	90	1900	2.45	3.0
Film C	950	100	1900	2.45	1.0

Table 2. Summary of the electrical and Raman results for the IIa diamond and films A, B, and C.

Sample	Mobility (cm^2 V^{-1} s^{-1}) at 200 V cm^{-1}	Lifetime (ps) at 200 V cm^{-1}	Collection distance *d* (μm) at 10 kV cm^{-1}	Raman FWHM (cm^{-1})
IIa	4000	300	30	2.4
Film A	50	50	<0.1	7.1
Film B	1000	100	2	4.8
Film C	4000	150	15	3.3

Because the average grain size of the polycrystalline CVD diamond films is comparable to the charge collection distance measured in these films, a large percentage of the charge carriers must be influenced by the grain boundaries. However, combined electron and hole mobilities for the CVD films are comparable to those measured in IIa diamonds and the dependence of the mobility and lifetime is also similar. This indicates that the mobility is not adversely affected by the grain boundaries in polycrystalline diamond films. This unexpected result along with the recent improvements in the electrical transport properties are encouraging findings in the development of diamond electronic devices. Fast, radiation-hard detectors for ionizing radiation may be among the first of such devices.

REFERENCES AND NOTES

1. S. F. Kozlov, R. Stuck, M. Hage-Ali, P. Siffert, *IEEE Trans. Nucl. Sci.* **NS-22**, 160 (1975).
2. M. I. Landstrass and D. M. Fleetwood, *Appl. Phys. Lett.* **56**, 2316 (1990).
3. G. Sh. Gildenblat, S. A. Grot, C. W. Hatfield, A. R. Badzian, T. Badzian, *IEEE Electron Device Lett.* **11**, 371 (1990).
4. M. N. Yoder, in *Applications of Diamond Films and Related Materials*, Y. Tzeng, M. Yoshikawa, M. Murakawa, A. Feldman, Eds. (Elsevier, Amsterdam, 1991), pp. 287–293.
5. M. W. Geis, D. D. Rathman, D. J. Ehrlich, R. A. Murphy, W. T. Lindley, *IEEE Electron Device Lett.* **8**, 341 (1987).
6. M. W. Geis, N. N. Efremow, D. D. Rathman, *J. Vac. Sci. Technol. A* **6**, 1953 (1988).
7. M. W. Geis, D. D. Rathman, M. Rothschild, in *SDIO/IST–ONR Diamond Technology Symposium Book of Abstracts* (Crystal City, VA, 1988), p. W15.
8. A. T. Collins, *Semicond. Sci. Technol.* **4**, 605 (1989).
9. M. Geis, *Proc. IEEE* **79**, 669 (1991).
10. G. Sh. Gildenblat, S. A. Grot, A. Badzian, *ibid.*, p. 647.
11. L. S. Pan *et al.*, *Science* **255**, 830 (1992).
12. L. S. Pan, unpublished material.
13. M. Kamo, Y. Sato, S. Matsumoto, N. Setaka, *J. Cryst. Growth* **62**, 642 (1983).
14. M. D. Drory and C. F. Gardinier, *J. Am. Ceram. Soc.* **74**, 3148 (1991).
15. D. R. Kania *et al.*, *J. Appl. Phys.* **68**, 124 (1990).
16. L. S. Pan, D. R. Kania, P. Pianetta, O. L. Landen, *Appl. Phys. Lett.* **57**, 623 (1990).
17. J. E. Graebner, S. Jin, G. W. Kammlott, J. A. Herb, C. A. Gardenier, *ibid.* **60**, 1576 (1992).
18. W. A. Yarbrough and R. Messier, *Science* **247**, 688 (1990).
19. R. J. Nemanich, L. Bergman, Y. M. LeGrice, R. E. Shroder, in *New Diamond Science and Technology* (Materials Research Society, Pittsburgh, 1991), p. 741.
20. J. W. Ager III, D. K. Veirs, G. M. Rosenblatt, *Phys. Rev. B* **43**, 6491 (1991).
21. This work was supported by the Superconducting Super Collider Laboratory at the Department of Energy, Strategic Defense Initiative Organization–Innovative Science and Technology, and the Army at Fort Monmouth. This work was partially performed under the auspices of the Department of Energy by Lawrence Livermore National Laboratories under contract W-7405-ENG-48 and by Lawrence Berkeley Laboratory under contract DE-AC03-76SF00098. Additional support came from the Texas National Research Laboratory Commission, Research and Development Program, and the Superconducting Super Collider Laboratory, Physics Research Division. One of the authors (S.H.) thanks the University of California Berkeley Microfabrication Laboratory technical staff for their assistance. We also thank J. Menendez for suggesting the interpretation of the Raman line shape in CVD films.

7 December 1992; accepted 19 February 1993

Experimental Evidence for a New Iron Phase and Implications for Earth's Core

S. K. Saxena, G. Shen, P. Lazor

Iron is known to occur in four different crystal structural forms. One of these, the densest form (ε phase, hexagonal close-packed) is considered to have formed Earth's core. Theoretical arguments based on available high-temperature and high-pressure iron data indicate the possibility of a fifth less dense iron phase forming the core. Study of iron phase transition conducted between pressures of 20 to 100 gigapascals and 1000 to 2200 Kelvin provides an experimental confirmation of the existence of this new phase. The ε iron phase transforms to this lower density phase before melting. The new phase may form a large part of Earth's core.

Iron has been thought to occur in four solid structural states: δ (body-centered-cubic, bcc), α (bcc), γ (face-centered-cubic, fcc), and ε (hexagonal close-packed, hcp). The ε phase has been considered to constitute the bulk of the solid inner core and, with some additional light elements (sulfur, for example, or oxygen), the liquid outer core (*1*). With the availability of new experimental data (*2–11*) and theoretical considerations (*3*), this model of the core has come under scrutiny. Currently available experimental data (*2–11*) on phase equilibrium relations from static devices (techniques with in situ heating of a sample under pressure over a period of time) are displayed in Fig. 1. The phase transition boundaries α-γ, γ-ε, and α-ε meet at one point, the so-called triple point; at such pressure and temperature all three forms of iron coexist in equilibrium. Recent theoretical study on iron properties at high pressure and high temperature by Anderson (*12*) has shown that determination of the ε-γ phase transformation and the ε-γ-melt triple point are particularly crucial in understanding the state of the Earth's core. The argument is that the pressure and temperature of the triple point determines the behavior of the melting curve at high pressures. Thermodynamically, the pressure-temperature slope of the ε-γ phase equilibrium curve constrains the estimated enthalpy, entropy, and other physical properties of the ε phase, which are largely unknown. With the availability of the equilibrium data on the ε-γ phase transformation, one may assess the thermodynamic properties of the ε phase, which in turn can be used in the estimation of the properties of the iron melt.

A triple point, similar to the one shown in Fig. 1, should exist for the coexisting γ, ε, and melt. Available experimental data on the ε-γ transition appear to indicate that such a triple point would be at about 2700 K and 60 to 70 GPa. The problem is that Brown and McQueen (*13*) located a solid-solid transition at 4400 ± 300 K at a pressure of 200 ± 2 GPa. This phase transition could not be the ε-γ transition; the triple point is located at too low a pressure for this to be possible. This apparent inconsistency between the sets of data led Boehler (*15*) to conclude that a fifth iron phase should exist; Ross *et al.* (*16*) and Young and Grover (*17*) indicated that such a phase is theoretically

Theoretical Geochemistry, Institute of Earth Sciences, Box 555, Uppsala University, S-752 36 Uppsala, Sweden.

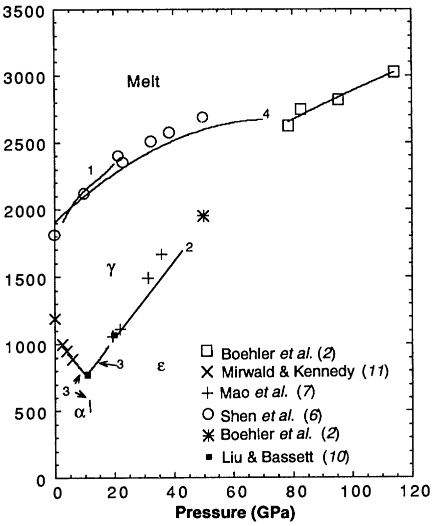

Fig. 1. Representative available experimental data on iron phase relations. Several sets of data below 10 GPa and the stability field of δ bcc phase have not been shown. The three iron phases α, γ, and ε are, respectively, the bcc (body-centered-cubic), fcc (face-centered-cubic), and hcp (hexagonal close-packed). Curve labeled 1 is from Liu and Bassett (*10*), 2 is from Boehler (*15*), 3 is from Bundy (*9*), and 4 is from Boehler *et al.* (*2*).